Theory for tunneling spectroscopy of anisotropic superconductors

Satoshi Kashiwaya
Electrotechnical Laboratory, Umezono, Tsukuba, Ibaraki 305, Japan

Yukio Tanaka
Niigata University, Igarashi, Niigata 950-21, Japan

Masao Koyanagi and Koji Kajimura
Electrotechnical Laboratory, Umezono, Tsukuba, Ibaraki 305, Japan

(Received 5 September 1995)

A theory for the tunneling spectroscopy of a normal-metal–insulator–anisotropic-superconductor (N-I-S) junction is presented. In anisotropic superconductors, the effective pair potential felt by the quasiparticles depends on their wave vectors in contrast to the case of isotropic s-wave superconductors. By introducing the effect into the Blonder-Tinkham-Klapwidjk formula, a conductance formula for N-I-S junctions is obtained. It is shown that the conductance spectra are a function not only of the amplitudes of pair potentials but also of their phases. Tunneling conductance spectra calculated for various symmetries strongly depend on the relation between the tunneling direction and crystalline axes. In some crystalline angle regions of d-wave superconductors, a zero-energy peak in the conductance spectra is calculated. This conductance peak reflects the existence of anomalous bound states around the insulator–anisotropic-superconductor interface. The relation between the tunneling conductance spectra and the local density of states of superconductors is discussed.

I. INTRODUCTION

Tunneling spectroscopy has been accepted to be one of the most sensitive probes of electronic states of superconductors. Its validity has been verified and established through many experimental and theoretical works.[1–2] However, they are based on the discussion about isotropic s-wave superconductors and the anisotropy of pair potential in $\mathbf{k}$ space has not been taken into account except in a few cases.[3–4]

Nowadays, the electronic structure of high-T_c superconductors is a controversial problem. There exist growing evidences for d-wave symmetry in the pair potential of high-T_c superconductors.[5–8] As for tunneling spectroscopy measurements, many groups have tried to clarify the gap structure, but their results are not yet converged. In addition to the gap structure, zero-bias conductance peaks (ZBCP's) are frequently observed, which cannot be explained in terms of traditional tunneling theories.[9–11] We believe that the main difficulty in this area ascribes to the lack of the theory to treat anisotropic superconductors. Koyama *et al.* calculated the quasiparticle transport between the normal-metal and d-wave superconductor, although their results are restricted to a special case.[12]

Recently, Hu[13] predicted the existence of dispersionless half filled states exactly at the Fermi level on the surface of a d_{xy}-wave superconductor (equivalent to the case when the a axis of a $d_{x^2-y^2}$-wave superconductor is tilted by $\pi/4$ from the surface normal). Later, we discussed the tunneling spectra of d-wave superconductors and showed the appearance of ZBCP's when the a axis of the $d_{x^2-y^2}$-wave superconductors are tilted from the surface normal.[14] The comparison between the experimental data of scanning tunneling microscopy (STM) and the theoretical calculation showed good agreement.[15] Anomalous surface states on the surface of d_{xy}-wave superconductors are also obtained by Green's function method.[16–18] All these results demand that we should restudy the tunneling spectroscopy for superconductors by correctly taking account of the surface states which are originated from the anisotropy of the pair potential.

In this paper, we will extensively investigate the tunneling conductance spectrum of a normal-metal–insulator–superconductor (N-I-S) junction for spin singlet anisotropic superconductors. One of the important purposes of this paper is to clarify what kind of physical quantities the tunneling spectroscopy is detecting. In Sec. II, a conductance formula for an N-I-S junction is derived. We will solve the Bogoliubov–de Gennes (BdG) equations for an anisotropic superconductor in an N-I-S configuration. Using a two-component wave-function description in the equations, the reflection amplitudes for electrons injected from the normal metal to the insulator are obtained. The conductance spectrum of the junction is calculated from the reflection amplitudes using the Blonder-Tinkham-Klapwidjk (BTK) formula.[19] In Sec. III, the physical origin of the conductance peaks is discussed. It is shown that the energy level giving the conductance peak is determined by a quantum condition of the bound quasiparticles in a pseudoquantum well. In Sec. IV, the tunneling conductance spectra are calculated for superconductors having different symmetries. The effect of the difference in Fermi wave numbers of the two electrodes is also discussed. In Sec. V, the tunneling conductance spectra are compared with the local density of states (LDOS) obtained by Green's function method. In Sec. VI, we will summarize our results.

Throughout this paper, the pair potentials are assumed to be spatially constant in superconductors, and the self-consistency of the spatial distribution in the pair potential is ignored for simplicity. The temperature is fixed to 0 K. The

Fermi wave numbers in N and S are assumed to be k_{FN} and k_{FS}, respectively. The effective mass m is assumed to be the same in the two electrodes. The impurity scattering in the system and random reflection at the interfaces are ignored.

II. CONDUCTANCE FORMULA

The conductance spectrum of the N-I-S junction is calculated from the reflection amplitudes of the electrons injected from the normal side. There are two types of reflection processes: (i) the injected electron is reflected as a hole (called as Andreev reflection process[20]); (ii) the electron is reflected as an electron (called as normal reflection process). To calculate the reflection amplitudes of the two processes, we start from the BdG equation for anisotropic superconductors.

In superconductors, the quasiparticles are expressed by two-component wave function $\Psi(\mathbf{r})$,

$$\Psi(\mathbf{r})=\begin{bmatrix} f(\mathbf{r}) \\ g(\mathbf{r}) \end{bmatrix}. \tag{1}$$

Using $f(\mathbf{r})$ and $g(\mathbf{r})$ the BdG equation is written as[4]

$$\begin{aligned} Ef(\mathbf{r}_1)&=\mathbf{h}_0(\mathbf{r}_1)f(\mathbf{r}_1)+\int d\mathbf{r}_2\ \Delta_a(\mathbf{r}_1,\mathbf{r}_2)g(\mathbf{r}_2), \\ Eg(\mathbf{r}_1)&=-\mathbf{h}_0(\mathbf{r}_1)g(\mathbf{r}_1)+\int d\mathbf{r}_2\ \Delta_a^*(\mathbf{r}_1,\mathbf{r}_2)f(\mathbf{r}_2). \end{aligned} \tag{2}$$

Here, Δ_a is a pair potential, $\mathbf{h}_0(\mathbf{r})=-\hbar^2\nabla_{\mathbf{r}}^2/2m-\mu+V(\mathbf{r})$, μ the chemical potential, $V(\mathbf{r})$ a Hartree potential in the N-I-S system, and E the energy measured from the Fermi energy E_F. These equations reduce to the usual Schrödinger equations in the absence of the pair potential. The pair potential used in the above equations is a function of two position coordinates $\mathbf{r}_1$ and $\mathbf{r}_2$, and can be transformed to

$$\Delta_b(\mathbf{s},\mathbf{r})=\Delta_a(\mathbf{r}_1,\mathbf{r}_2), \tag{3}$$

where $\mathbf{s}=\mathbf{x}-\mathbf{x}'$ and $\mathbf{r}=(\mathbf{x}+\mathbf{x}')/2$. In the Fourier transformed form for s,

$$\Delta_c(\mathbf{k},\mathbf{r})=\int \mathbf{ds}\ \exp(-i\mathbf{ks})\Delta_b(\mathbf{s},\mathbf{r}). \tag{4}$$

In the weak coupling limit, the wave vector $\mathbf{k}$ is fixed on the Fermi surface,

$$\Delta(\boldsymbol{\gamma},\mathbf{r})=\Delta_c(\mathbf{k},\mathbf{r}), \tag{5}$$

where $\boldsymbol{\gamma}$ is a unit vector,

$$\boldsymbol{\gamma}=\frac{\mathbf{k}}{|\mathbf{k}|}=\frac{\mathbf{k}}{k_{\mathrm{FS}}}. \tag{6}$$

Thus the pair potential is transformed into the function of the position and the direction of the traveling quasiparticle. Using $\Delta(\boldsymbol{\gamma},\mathbf{r})$, the BdG equations for anisotropic superconductors are approximated as

$$\begin{aligned} Ef(\boldsymbol{\gamma},\mathbf{r})&=h_0(\mathbf{r})f(\boldsymbol{\gamma},\mathbf{r})+\Delta(\boldsymbol{\gamma},\mathbf{r})g(\boldsymbol{\gamma},\mathbf{r}), \\ Eg(\boldsymbol{\gamma},\mathbf{r})&=-h_0(\mathbf{r})g(\boldsymbol{\gamma},\mathbf{r})+\Delta^*(\boldsymbol{\gamma},\mathbf{r})f(\boldsymbol{\gamma},\mathbf{r}). \end{aligned} \tag{7}$$

To avoid atomic-scale oscillation, we use two envelope functions, $u(\boldsymbol{\gamma},\mathbf{r})$ and $\nu(\boldsymbol{\gamma},\mathbf{r})$,

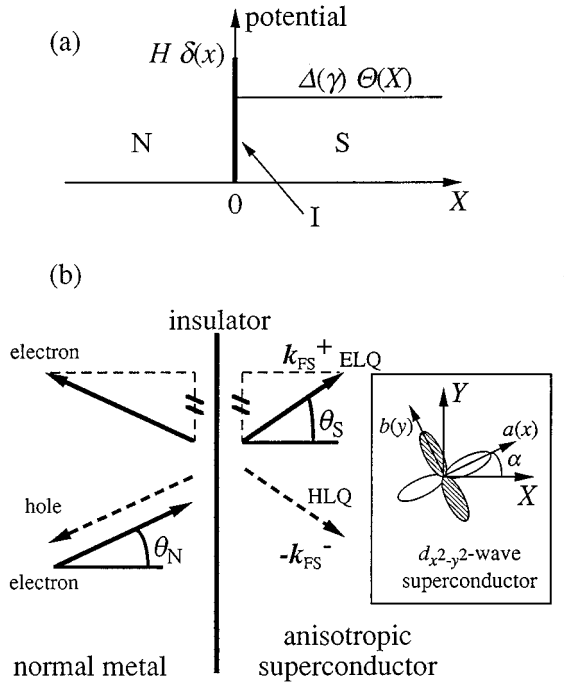

FIG. 1. (a) Potential model of N-I-S junction used in the calculation. The insulator is described by a δ function whose amplitude is H. The pair potential is expressed by $\Delta(\gamma)\Theta(X)$ where $\Theta(X)$ is the a Heaviside-step function. (b) Schematic illustration of transmission and reflection processes in the N-I-S junction. The wave-vector components parallel to the interface are conserved for all the processes. Since electronlike quasiparticles (ELQ) and holelike quasiparticles (HLQ) have different wave vectors ($\mathbf{k}_{\mathrm{FS}}^{+}$ and $\mathbf{k}_{\mathrm{FS}}^{-}$), they experience different effective pair potentials. The inset shows the pair potential for a $d_{x^2-y^2}$-wave superconductor in the case of ab-plane tunneling (see Sec. IV and Fig. 9).

$$\begin{aligned} f(\boldsymbol{\gamma},\mathbf{r})&=u(\boldsymbol{\gamma},\mathbf{r})\exp(ik_{\mathrm{FS}}\boldsymbol{\gamma}\cdot\mathbf{r}), \\ g(\boldsymbol{\gamma},\mathbf{r})&=\nu(\boldsymbol{\gamma},\mathbf{r})\exp(ik_{\mathrm{FS}}\boldsymbol{\gamma}\cdot\mathbf{r}). \end{aligned} \tag{8}$$

In the framework of a quasiclassical approximation, we obtain the BdG equations as

$$\begin{aligned} \frac{\partial u(\boldsymbol{\gamma},\mathbf{r})}{\partial\mathbf{r}}&=\left(\frac{-i\hbar^2k_F}{m}\right)^{-1}\boldsymbol{\gamma}[\{E-V(\mathbf{r})\}u(\boldsymbol{\gamma},\mathbf{r}) \\ &\quad-\Delta(\boldsymbol{\gamma},\mathbf{r})\nu(\boldsymbol{\gamma},\mathbf{r})], \\ \frac{\partial\nu(\boldsymbol{\gamma},\mathbf{r})}{\partial\mathbf{r}}&=\left(\frac{i\hbar^2k_F}{m}\right)^{-1}\boldsymbol{\gamma}[\{E-V(\mathbf{r})\}\nu(\boldsymbol{\gamma},\mathbf{r}) \\ &\quad-\Delta^*(\boldsymbol{\gamma},\mathbf{r})u(\boldsymbol{\gamma},\mathbf{r})]. \end{aligned} \tag{9}$$

Figure 1(a) shows the schematic illustration of the N-I-S junction used here. The interfaces are assumed to be perfectly flat, and the X axis is taken to be parallel to the normal of the interface. The barrier potential is located at $X=0$, and

assumed to have a delta-functional form $H\delta(X)$. The pair potential has a step function form $\Delta(\gamma)\Theta(X)$, where $\Theta(X)$ is the Heaviside step function. Suppose an electron having a wave vector with angle θ_N to the interface normal ($-\pi/2<\theta_N<\pi/2$) and energy E is injected from the normal side. Four trajectories are possible: (a) reflected as holes, (b) reflected as electrons, (c) transmitted to the superconductor as electronlike quasiparticles (ELQ), and (d) transmitted to the superconductor as holelike quasiparticles (HLQ). Since the system has a translational invariance for the direction parallel to the interface, the wave-vector components along these directions are conserved. All the above trajectories are on the same plane, which we define as XY plane as shown in Fig. 1(b). The wave-vector components out of the plane for all the trajectories become zero. As a result, the three-dimensional motion reduces to the two-dimensional one. Since the ELQ and HLQ have different wave vectors ($\mathbf{k}_{\rm FS}^{+}$ and $-\mathbf{k}_{\rm FS}^{-}$, respectively), they feel different effective pair potentials Δ_+ and Δ_-, respectively,

$$\Delta_{\pm}\equiv\Delta(\pm\mathbf{k}_{\rm FS}^{\pm}/k_{\rm FS})=|\Delta_{\pm}|\exp(i\varphi_{\pm}), \tag{10}$$

where φ_+ and φ_- are the phases of the effective pair potentials. The reflection coefficients are obtained by solving the BdG equation, Eq. (9), under the boundary condition,

$$\begin{aligned}&\Psi_S(\mathbf{r})|_{X=0+}=\Psi_N(\mathbf{r})|_{X=0-}\\ &\left.\frac{d\Psi_S(\mathbf{r})}{dx}\right|_{X=0+}-\left.\frac{d\Psi_N(\mathbf{r})}{dx}\right|_{X=0-}=\frac{2mH}{\hbar^2}\,\Psi_S(\mathbf{r})|_{X=0+},\end{aligned} \tag{11}$$

where

$$\begin{aligned}\Psi_N(\mathbf{r})&=e^{ik_{\rm FN}^{+}r}\begin{pmatrix}1\\0\end{pmatrix}+a(E)e^{ik_{\rm FN}^{-}r}\begin{pmatrix}0\\1\end{pmatrix}+b(E)e^{-ik_{\rm FN}^{+}r}\begin{pmatrix}1\\0\end{pmatrix},\\ \Psi_S(\mathbf{r})&=c(E)e^{ik_{\rm FS}^{+}r}\begin{pmatrix}\sqrt{E+\Omega_+/2E}\\ e^{-i\varphi_+}\sqrt{E-\Omega_+/2E}\end{pmatrix}\\ &\quad+d(E)e^{-ik_{\rm FS}^{-}r}\begin{pmatrix}e^{i\varphi_-}\sqrt{E-\Omega_-/2E}\\ \sqrt{E+\Omega_-/2E}\end{pmatrix},\end{aligned} \tag{12}$$

$$|\mathbf{k}_{\rm FN}^{\pm}|=\sqrt{k_{\rm FN}^2\pm\frac{2mE}{\hbar^2}}\approx k_{\rm FN},\quad |\mathbf{k}_{\rm FS}^{\pm}|=\sqrt{k_{\rm FS}^2\pm\frac{2m\Omega_{\pm}}{\hbar^2}}\approx k_{\rm FS},$$

$$\Omega_{\pm}=\sqrt{E^2-|\Delta_{\pm}|^2}.$$

The ratio of Fermi wave number λ_0 is defined by

$$\lambda_0\equiv\frac{k_{\rm FS}}{k_{\rm FN}}. \tag{13}$$

The momentum conservation law for Y direction is written as

$$k_{\rm FS}\sin\theta_S=k_{\rm FN}\sin\theta_N, \tag{14}$$

where $-\pi/2<\theta_S<\pi/2$. When $\lambda_0<1$, total reflection takes place at the N-I interface for $|\theta_N|>\sin^{-1}\lambda_0$. Coefficients of the Andreev reflection process $a(E)$ and the normal reflection process $b(E)$ for a given θ_N are expressed as

$$\begin{aligned}a(E)&=\frac{4\lambda\Gamma_+\exp(-i\varphi_+)}{(1+\lambda)^2+4Z^2-\{(1-\lambda)^2+4Z^2\}\Gamma_+\Gamma_-\exp(i\varphi_--i\varphi_+)},\\ b(E)&=\frac{-(1-\lambda^2-4iZ-4Z^2)\{1-\Gamma_+\Gamma_-\exp(i\varphi_--i\varphi_+)\}}{(1+\lambda)^2+4Z^2-\{(1-\lambda)^2+4Z^2\}\Gamma_+\Gamma_-\exp(i\varphi_--i\varphi_+)},\end{aligned} \tag{15}$$

where

$$\Gamma_{\pm}=\frac{E-\Omega_{\pm}}{|\Delta_{\pm}|},\quad \lambda=\lambda_0\frac{\cos\theta_S}{\cos\theta_N},\quad Z=\frac{Z_0}{\cos\theta_N},$$

$$Z_0=\frac{mH}{\hbar^2k_{\rm FN}}.$$

According to the BTK formula, the conductance of the junction $\sigma_S(E)$ is calculated from the probability amplitudes of the two processes,[19]

$$\sigma_S(E)=1+|a(E)|^2-|b(E)|^2. \tag{16}$$

This formulation is a revised version of the Landauer-type formulation of conductance for an N-S structure.[21,22] Using this relation, the conductance $\sigma_S(E)$ for a given θ_N is written as

$$\sigma_S(E)=\sigma_N\frac{1+\sigma_N|\Gamma_+|^2+(\sigma_N-1)|\Gamma_+\Gamma_-|^2}{|1+(\sigma_N-1)\Gamma_+\Gamma_-\exp(i\varphi_--i\varphi_+)|^2}, \tag{17}$$

where

$$\sigma_N\equiv\frac{4\lambda}{(1+\lambda)^2+4Z^2}. \tag{18}$$

Here, σ_N is the conductance for an N-I-N junction in the same geometrical configuration and indicates the probability distribution of tunneling electrons in k space. Equation (17) reduces to the BTK formula by setting $\Gamma_+=\Gamma_-$ and $\varphi_+=\varphi_-$. Since Eq. (17) is not symmetric with respect to the exchange of the suffix $+$ and $-$, the conductance spectra $\sigma_S(E)$ is not symmetric for injection angles θ_N and $-\theta_N$.

We define two types of conductance spectra for convenience. The normalized conductance spectrum $\sigma_R(E)$ is defined for a fixed θ_N,

$$\sigma_R(E)=\frac{\sigma_S(E)}{\sigma_N}=\frac{1+\sigma_N|\Gamma_+|^2+(\sigma_N-1)|\Gamma_+\Gamma_-|^2}{|1+(\sigma_N-1)\Gamma_+\Gamma_-\ \exp(i\varphi_--i\varphi_+)|^2}. \tag{19}$$

Although $\sigma_R(E)$ is a function of E, σ_N, Δ_+, and Δ_-, it can also be regarded as a function of E and θ_N in a given junction configuration, i.e., for given Z_0, λ_0, and the pair potential form of the superconductor. In a real N-I-S junction configuration, total tunneling conductance spectrum $\sigma_T(E)$ includes the integration over the solid angle,

$$\sigma_T(E)=\frac{\int d\omega\ \sigma_S(E)\cos\chi}{\int d\omega\ \sigma_N\cos\chi}=\frac{\int d\omega\ \sigma_N\cos\chi\sigma_R(E)}{\int d\omega\ \sigma_N\cos\chi}. \tag{20}$$

Here, χ is the angle between ω and X axis, and the integration is performed over the Fermi surface (half-sphere). In the case of two dimension, it reduces to the integration over the injection angle θ_N,

$$\sigma_T(E)=\frac{\int_{-\pi/2}^{\pi/2}d\theta_N\ \sigma_S(E)\cos\theta_N}{\int_{-\pi/2}^{\pi/2}d\theta_N\ \sigma_N\cos\theta_N}=\frac{\int_{-\pi/2}^{\pi/2}d\theta_N\ \sigma_N\cos\theta_N\sigma_R(E)}{\int_{-\pi/2}^{\pi/2}d\theta_N\ \sigma_N\cos\theta_N}. \tag{21}$$

Note that $\sigma_T(E)$ can be regarded as the expectation value of $\sigma_R(E)$ with the probability distribution of $\sigma_N\cos\theta_N$.[23]

It is important to note that the tunneling conductance spectrum depends not only on the amplitudes but also on the phases of pair potentials. The effect of the phase has long been overlooked, because most theories are based on isotropic s-wave superconductors.

III. PEAK IN CONDUCTANCE SPECTRA

In this section, the conductance spectra $\sigma_R(E)$ are calculated by setting Δ_+, Δ_-, and Z values *a priori*, and the physical origin of the peak in the conductance spectra is discussed. Throughout this section, we assume $k_{\rm FN}=k_{\rm FS}$ ($\lambda_0=1$), where σ_N and $\sigma_R(E)$ are written as

$$\sigma_N=\frac{1}{1+Z^2}, \tag{22}$$

$$\sigma_R(E)=\frac{(1+Z^2)\{1+|\Gamma_+|^2+Z^2(1-|\Gamma_+\Gamma_-|^2)\}}{|1+Z^2\{1-\Gamma_+\Gamma_-\ \exp(i\varphi_--i\varphi_+)\}|^2}. \tag{23}$$

Figures 2 shows $\sigma_R(E)$ when (a) $\Delta_+=\Delta_-=\Delta_0$ and (b) $\Delta_+=-\Delta_-=\Delta_0$ for various Z values. In both cases, $\sigma_R(E)$ equals 2 for $E<|\Delta_0|$ when $Z=0$, which means that the Andreev reflection takes place with the probability amplitude 1. With the increment of Z, the peak structures emerge. For the case (a), $\sigma_R(E)$ has energy gap structure whose shape is similar to the BCS density of states (DOS) having a sharp peak at Δ_0 and clear gap below Δ_0. However, in the case (b), when the signs of Δ_+ and Δ_- are opposite, a peak appears at zero-energy level. It becomes sharper and higher with increase of Z, and diverges in the large Z limit. The latter spectra are completely different from what we expect for superconductors based on conventional tunneling theory.

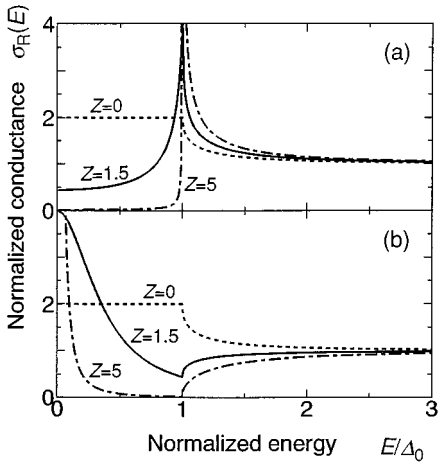

FIG. 2. Calculated $\sigma_R(E)$ for $Z=0$, 1.5, and 5 when (a) $\Delta_+=\Delta_-=\Delta_0$ and (b) $\Delta_+=-\Delta_-=\Delta_0$. As Z becomes larger, peak structures are enhanced. The peak exists at Δ_0 in (a) and at zero energy in (b).

From the condition that the numerator of Eq. (23) diverges for large Z, the equation giving the peak energy level E_p is written as

$$\Gamma_+\Gamma_-|_{E=E_p}=\exp(i\varphi_+-i\varphi_-). \tag{24}$$

Under this condition, the conductance $\sigma_S(E=E_p)=2$ independent of Z value, that is, the tunneling probability is not influenced by the barrier height at $E=E_p$ just like the resonance tunneling process.[14,24] Then, the peak height $\sigma_R(E)$ at $E=E_p$ is $2(1+Z^2)$ which diverges in the limit of large barrier height. In this limit, we can estimate $\sigma_R(E)\to 0$ when $E<\min\{|\Delta_+|,\ |\Delta_-|\}$ and $E\neq E_p$, and $\sigma_R(E)\to 1$ when $E\gg|\Delta_+|$ and $E\gg|\Delta_-|$.

Next, we discuss the physical meaning of Eq. (24) using a simple model. Suppose a one-dimensional superconductor–normal-metal–superconductor (S-N-S) structure in which the pair potentials of superconductors are $\Delta_+=|\Delta_+|\exp(i\varphi_+)$ and $\Delta_-=|\Delta_-|\exp(i\varphi_-)$, respectively. The width of the normal region is assumed to be d_n. The quasiparticles in the pseudoquantum well (normal region) are confined if their energies are less than the amplitudes of both pair potentials ($E<\min\{|\Delta_+|,\ |\Delta_-|\}$).[25–29] The bound quasiparticles travels along a closed path by repeating the Andreev reflections at S-N interfaces. The Andreev reflection accompanies energy dependent phase shift through the reflection process. By summing up the phase shift along one round of the closed path, we obtain a quantum condition of the phase for the bound quasiparticles,[28,29]

$$-\arctan\left(\frac{\sqrt{|\Delta_+|^2-E^2}}{E}\right)-\arctan\left(\frac{\sqrt{|\Delta_-|^2-E^2}}{E}\right)-\varphi_d+2\varphi_N=2j\pi. \tag{25}$$

Here, $\varphi_d=\varphi_+-\varphi_-$, $\varphi_N=md_nE/(\hbar^2k_{\rm FN})$, and j is an integer. This condition is the generalization of that for de Gennes–Saint James bound states[30,31] and reduces to Eq. (b) of Table I in Ref. 15 by setting $|\Delta_+|=|\Delta_-|$. When $\varphi_d=\pi$, Eq. (25) is satisfied by $E=0$ independent of σ_N (midgap states).[13] When the normal region thickness is zero ($d_n=\varphi_N=0$), Eq. (25)

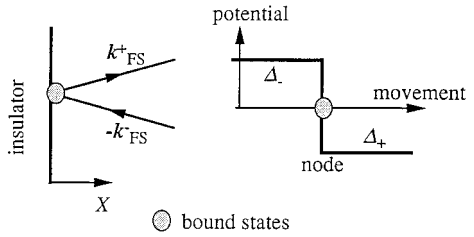

FIG. 3. Quasiparticle trajectory around I-S interface. The injected quasiparticle from the bulk is elastically reflected at the insulator. Accordingly, the effective pair potential felt by the quasiparticle changes. The bound states are formed at the node of pair potentials.

becomes equivalent to Eq. (24). Based on these considerations, the physical origin of the conductance peak is interpreted as follows. The quasiparticles injected from the bulk of the superconductor to the I-S interface are elastically reflected at the interface. The quasiparticles change their wave vectors through the reflections from $-\mathbf{k}_{FS}^{-}$ to $\mathbf{k}_{FS}^{+}$ (Fig. 3). Accordingly, the effective pair potential felt by them also changes from $\Delta(-\mathbf{k}_{FS}^{-})=\Delta_-$ to $\Delta(\mathbf{k}_{FS}^{+})=\Delta_+$ at the insulator. The interface can be regarded as the node of pair potential for the quasiparticles, and the bound states are formed at the node whose energy level is given by Eq. (24). The tunneling electrons from N to S flow via the bound states just like the resonant tunneling process. Thus the conductance peak is formed at the energy levels of the bound states.

Next we discuss the dependence of $\sigma_R(E)$ and the bound state level (E_p) as a function of the phase difference φ_d ($0<\varphi_d<2\pi$). Figure 4 shows the dependence of E_p on φ_d when $|\Delta_+|=|\Delta_-|=\Delta_0$. In the case of $\varphi_d=0$, the bound states are formed at Δ_0. As φ_d increases toward π, the bound state level becomes lower toward 0. When φ_d exceeds π, the bound state level moves beneath the Fermi level, and does not contribute to the current flow. Figure 5 shows the normalized conductance spectra $\sigma_R(E)$ corresponding to the phase difference (a)–(d) in Fig. 4 when $Z=5$. The spectrum 4(a) has the form of BCS DOS. As φ_d becomes larger [curves 4(b) and 4(c)], the peak position moves toward the zero energy. Then, the peak disappears when φ_d exceeds π [curves 4(d)]. Figure 6 shows the bound state levels as a

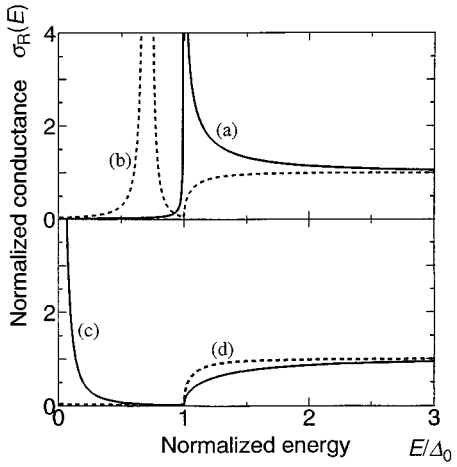

FIG. 5. Normalized conductance spectra $\sigma_R(E)$ as a function of φ_d in the case of $|\Delta_1|=|\Delta_2|=\Delta_0$; (a) $\varphi_d=0$, (b) $\varphi_d=\pi/2$, (c) $\varphi_d=\pi$, and (d) $\varphi_d=3\pi/2$. The peak energy levels clearly correspond to the bound states shown in Fig. 4. For the case of $\varphi_d>\pi$, the bound states move beneath the Fermi level, then the peak structures in the spectra disappear.

function of φ_d when the amplitudes of the two pair potentials are different ($2|\Delta_+|=|\Delta_-|=\Delta_0$). Since the energy level of the bound states must satisfy $E_p<\min\{|\Delta_+|, |\Delta_-|\}$, they exist only when $\pi/3<\varphi_d<5\pi/3$. Figure 7 shows the normalized conductance spectra $\sigma_R(E)$ corresponding to the lines in Fig. 6. It is important to note that, when $\varphi_d=\pi$, the bound states exist at zero-energy level independently from of the amplitude of pair potentials reflecting the existence of midgap states.[13]

The above bound states converge to the surface states in the large barrier-height limit. As will be verified in Sec. V, the surface states differ from the bulk states except when $\Delta_+=\Delta_-$. Now, the physical origin of surface states is clear. In anisotropic superconductors, different pair potentials are folded in k space. The quasiparticles change their wave vectors at the surface. Accordingly the effective pair potential felt by the quasiparticles also change at there. Then the bound states are formed between the two different pair potentials, that is, the effective pair potentials before and after the reflection. Of course, equivalent effects are expected to

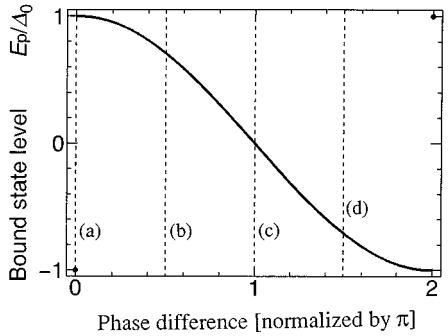

FIG. 4. Dependence of the bound state level on φ_d in the case of $|\Delta_1|=|\Delta_2|=\Delta_0$. When $\varphi_d=\pi$, the bound states are formed just at zero-energy level (midgap states). In the cases of $\varphi_d=0$ and 2π, the bound states exist at $\pm\Delta_0$. As for lines (a)–(d), see text and Fig. 5.

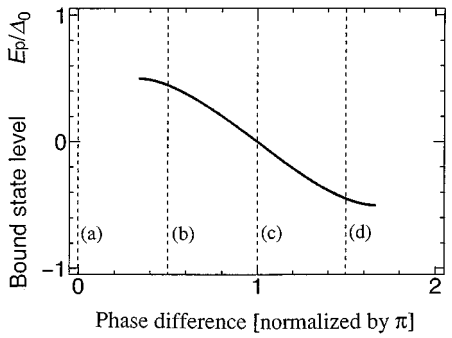

FIG. 6. Dependence of bound state levels on φ_d in the case of $2|\Delta_+|=|\Delta_-|=\Delta_0$. The bound states exist only when $\pi/3<\varphi_d<5\pi/3$. When $\varphi_d=\pi$, the bound states are formed just at zero-energy level (midgap states). As for lines (a)–(d), see text and Fig. 7.

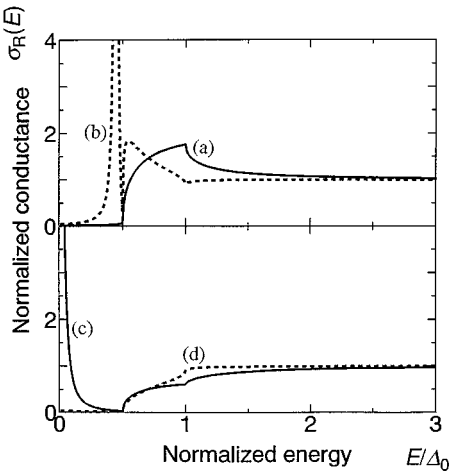

FIG. 7. Normalized conductance spectra $\sigma_R(E)$ as a function of φ_d in the case of $|\Delta_+|=2|\Delta_-|=\Delta_0$; (a) $\varphi_d=0$, (b) $\varphi_d=\pi/2$, (c) $\varphi_d=\pi$, and (d) $\varphi_d=3\pi/2$. Appearance of the peak in $\sigma_R(E)$ coincides with that of the bound states as shown in Fig. 6.

occur in various situations, such as, around the non-magnetic impurities and inside the vortex cores.[29]

IV. CONDUCTANCE SPECTRA FOR VARIOUS SYMMETRIES

The total tunneling conductance spectra $\sigma_T(E)$ of an N-I-S junction include the integration over the injection angle. In this section, $\sigma_T(E)$ is actually calculated for various symmetries in real junction configurations. In view of high-T_c superconductors, we restrict ourselves to two-dimensional symmetric superconductors. In such case, the effective pair potential is a function of k_x and k_y, where k_i ($i=x, y$ and z) is the i component of the wave vector $\mathbf{k}$. The functional
form used here is s wave $\{\Delta(\mathbf{k})=\Delta_1\}$, $d_{x^2-y^2}$ wave $\{\Delta(\mathbf{k})=\Delta_1\cos 2\theta_a\}$, extended s wave $\{\Delta(\mathbf{k})=\Delta_1+\Delta_2\cos 4\theta_a\}$, and $s+id_{x^2-y^2}$ wave $\{\Delta(\mathbf{k})=\Delta_1+i\Delta_2\cos 2\theta_a\}$. Here, θ_a is the angle between a axis and the vector $(k_x,k_y,0)$. There is nothing to say that the calculation is naturally extended to general three-dimensional superconductors. Throughout this section, it is assumed that the barrier has the delta-function form ($Z_0=5$). Although the effect of Fermi-wave number difference in the two electrodes is discussed in the latter part of this section, $\lambda_0=1$ is assumed unless described explicitly.

Suppose that the tunneling direction is parallel to the c axis of the crystal (c-axis tunneling). Since the wave-vector components parallel to the interface are conserved, $\Delta_+=\Delta_-$ is satisfied independent of injection angle for all the symmetries mentioned above. Then $\sigma_R(E)$ for a fixed θ_N has the form similar to the BCS DOS as shown in Fig. 5(a). In this case, we can easily understand that $\sigma_T(E)$ converges to the bulk DOS in the limit of large barrier height ($Z_0\to\infty$). Figure 8 shows the calculated $\sigma_T(E)$ of the c-axis tunneling for various symmetries. The gap structure in $\sigma_T(E)$ ascribes to the distribution of the superconducting gap in $\mathbf{k}$ space. In the case of $d_{x^2-y^2}$-wave superconductors, the well-known V-shaped gap structure is obtained.

Next, we assume that the tunneling direction is in the ab plane (ab-plane tunneling) of the superconductors as shown in the inset of Fig. 1(b). In this case, the integration is done in the two-dimensional Fermi surface for simplicity. Since $\Delta_+=\Delta_-$ is not generally satisfied, various types of $\sigma_T(E)$ are expected. Especially, the spectra depend strongly on α which is the angle between a axis and the interface normal ($-\pi/2<\alpha<\pi/2$). For $d_{x^2-y^2}$-wave superconductors with given θ_N, $\Delta_+=\Delta_1\cos 2(\theta_S-\alpha)$ and $\Delta_-=\Delta_1\cos 2(-\theta_S-\alpha)$. If α is zero or π, $\Delta_-=\Delta_+$ applies for all θ_N. Otherwise, the signs of Δ_+ and Δ_- are opposite for some θ_N region. When $\alpha=\pi/4$, their signs are opposite for all θ_N. In such cases, the zero-energy peak appears in $\sigma_T(E)$. Figure 9 shows the calculated $\sigma_T(E)$ of $d_{x^2-y^2}$-wave superconductors when $\alpha=0$, $\pi/8$, $\pi/4$. The zero-energy peak is clearly reproduced. The inset of Fig. 9 shows the dependence of zero-energy peak height on α. The peak height is enhanced as α varies form 0, and has a maximum at $\alpha=\pm\pi/4$. The peak height reflects the amount of θ_N, where the signs of Δ_+ and Δ_- are opposite, in the integral region $\pm\pi/2$. The spectra for d_{xy}-wave symmetry are calculated by simply adding $\pi/4$ to α. For the extended s-wave superconductors, $\sigma_T(E)$ drastically changes whether $\Delta_1>\Delta_2$ or not. Figure 10 shows the spectra when $\Delta_1>\Delta_2$ and $\Delta_1<\Delta_2$ with $\alpha=\pi/8$. Only in the latter case, the pair potential changes its sign in k space. As the result, the zero-energy peak appears only in the latter case. For the $s+id_{x^2-y^2}$-wave superconductors, since $\Delta_+=\Delta_1$

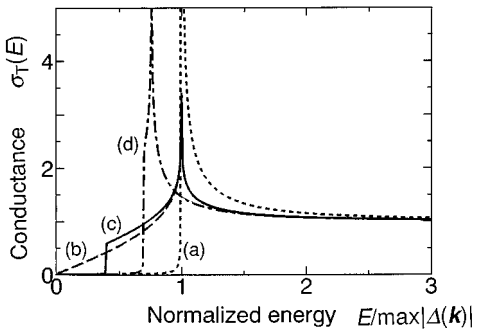

FIG. 8. Conductance spectra $\sigma_T(E)$ of c-axis tunneling for various symmetries: (a) s wave with $\Delta_1=\Delta_0$; (b) $d_{x^2-y^2}$ wave with $\Delta_1=\Delta_0$; (c) extend s wave with $\Delta_1=0.7\Delta_0$ and $\Delta_2=0.3\Delta_0$; (d) $s+id_{x^2-y^2}$ wave with $\Delta_1=0.7\Delta_0$ and $\Delta_2=0.3\Delta_0$.

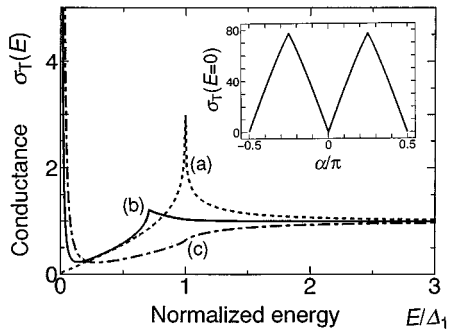

FIG. 9. Conductance spectra $\sigma_T(E)$ for the $d_{x^2-y^2}$ wave superconductor in the case of (a) $\alpha=0$, (b) $\pi/8$, and (c) $\pi/4$. The inset shows the dependence of zero-bias peak height on α. The peak height has maximum at $\alpha=\pm\pi/4$.

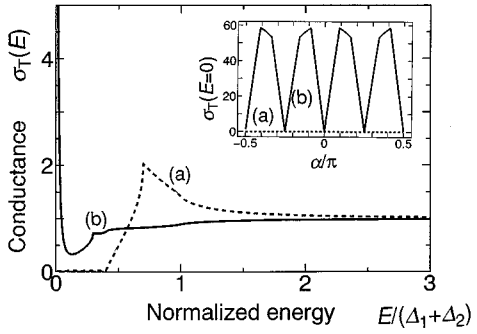

FIG. 10. Conductance spectra $\sigma_T(E)$ for the extended s-wave superconductor in the case of $\alpha=\pi/8$. The pair potentials are (a) $\Delta_1=0.7\Delta_0$ and $\Delta_2=0.3\Delta_0$, and (b) $\Delta_1=0.3\Delta_0$ and $\Delta_2=0.7\Delta_0$. The inset shows the dependence of zero-bias peak height on α.

$+i\Delta_2\cos 2(\theta_S-\alpha)$, and $\Delta_-=\Delta_1+i\Delta_2\cos 2(-\theta_S-\alpha)$, the phase difference between the two pair potentials is not restricted to a multiple of π. Thus the peak position moves between 0 and $\min\{|\Delta_+|,|\Delta_-|\}$ depending on the relation of Δ_+, Δ_- and α. Figure 11 shows $\sigma_T(E)$ for the $s+id_{x^2-y^2}$-wave superconductors with $\alpha=\pi/4$. In this case, the peaks exist at the energy levels corresponding to the amplitude of s-wave components.

Finally, we discuss the effect of the Fermi-wave number difference in the two electrodes. As stated previously, the wave vector component parallel to the interface is conserved through the tunneling process. As a result, the effective Fermi surface contributing to the electron transfer from N to S is restricted.[32] Figure 12 shows the schematic illustration of the Fermi surface of the two electrodes and the shaded regions correspond to the effective Fermi surface. The distribution of tunneling electron probability (expressed by distribution of σ_N) is finite only in the shaded region. The inset in Fig. 13 shows the dependence of σ_N on θ_S for various λ_0. In the case of $\lambda_0<1$, total reflection ($\sigma_N=0$) occurs at the N-I interface when the injection angle is larger than $\sin^{-1}(\lambda_0)$. However, this component has no serious effect on the dependence of σ_N and θ_S. On the contrary, when $\lambda_0>1$, the dependence of σ_N on θ_S is seriously affected by the value of λ_0. As λ_0 increases from 1, the directionality is enhanced. That is,

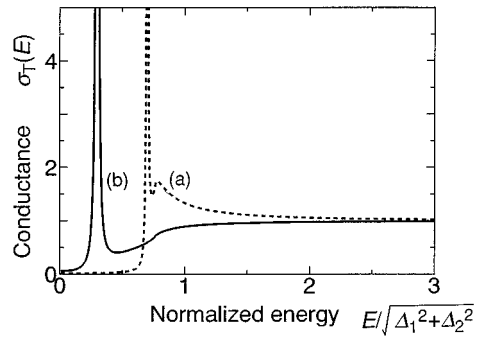

FIG. 11. Conductance spectra $\sigma_T(E)$ for the $s+id_{x^2-y^2}$ wave superconductor in the case of $\alpha=\pi/4$. The pair potentials are (a) $\Delta_1=0.7\Delta_0$ and $\Delta_2=0.3\Delta_0$, and (b) $\Delta_1=0.3\Delta_0$ and $\Delta_2=0.7\Delta_0$. The peaks exist at the energy levels corresponding to the amplitudes of s-wave components.

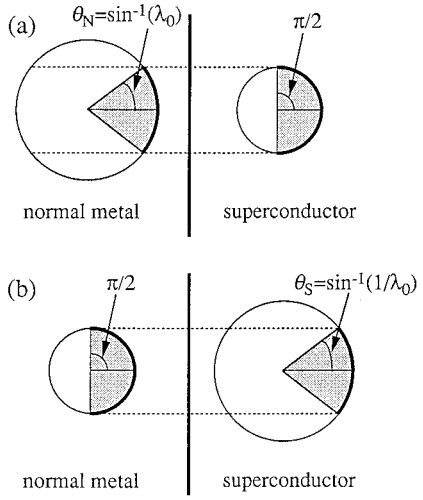

FIG. 12. Schematic illustration of the Fermi surface in both electrodes. To conserve the wave vector component parallel to the interface, the effective Fermi surface is restricted to shaded region with (a) $\lambda_0<1$ and (b) $\lambda_0>1$.

the distribution of tunneling electrons come to concentrate on the region that satisfies $\theta_S<\sin^{-1}(1/\lambda_0)$. The total tunneling conductance spectrum $\sigma_T(E)$ is influenced by λ_0 mainly through the dependence of σ_N on θ_s. Figure 13 shows $\sigma_T(E)$ for the ab-plane tunneling of the $d_{x^2-y^2}$-wave superconductor with $\alpha=0$. Clearly, the effect of Fermi-wave number difference is serious only in case of $\lambda_0>1$. As λ_0 increases from 1, the directionality of tunneling probability becomes prominent and the gap structure in $\sigma_T(E)$ comes to have a flat bottom.

V. TUNNELING SPECTRA AND LOCAL DENSITY OF STATES

The tunneling conductance spectrum has long been regarded to reflect the bulk DOS of the superconductors. In the previous section, we have shown the existence of bound states at the I-S interface of the anisotropic superconductors. It is revealed that the tunneling spectroscopy is seriously affected by the bound states, and unable to observe the bulk states. At this stage, there arises another question what kind

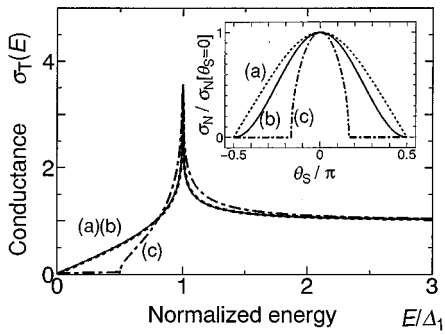

FIG. 13. Conductance spectra $\sigma_T(E)$ for $d_{x^2-y^2}$ wave superconductors with $\alpha=0$; (a) $\lambda_0=0.5$, (b) $\lambda_0=1$, and (c) $\lambda_0=2$. The inset shows the dependence of σ_N on θ_S.

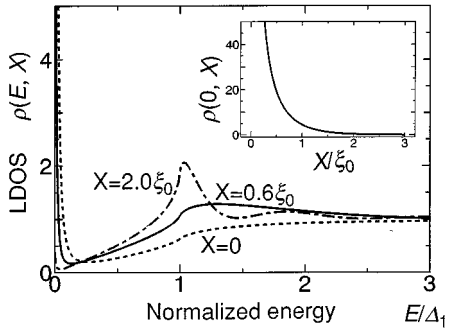

FIG. 14. Local density of states of a N-I-S junction of the $d_{x^2-y^2}$ wave superconductor with an ab-plane tunneling configuration ($\alpha=\pi/4$, $Z_0=5$): (a) $X=0$, (b) $X=0.6\xi_0$, and (c) $X=2\xi_0$. The inset shows the spatial dependence of zero-bias level $\rho(E=0, X)$. The zero-energy states decay into the bulk with length scale ξ_0.

of physical quantity the tunneling spectroscopy is detecting. To clarify it, we compare the conductance spectra with the LDOS in the N-I-S junction configuration, and discuss the relation lying between those two physical quantities.

The normalized LDOS $\rho_T(E,X)$ of S side of the N-I-S junction [shown in Fig. 1(a)] is calculated by Green's function method. The insulator is assumed to have a delta-function potential form and $\lambda_0=1$. In the case of two dimension, LDOS is given by[18]

$$\rho_T(E,X)=\frac{1}{\pi}\int_{-\pi/2}^{\pi/2} d\theta_S\ \rho(E,X), \quad X>0, \tag{26}$$

where

$$\rho(E,X)=\mathrm{Re}\left[\frac{E}{2\Omega_+}\left\{1+F_+\ \exp\left(\frac{2iX}{\xi_+}\right)\right\} + \frac{E}{2\Omega_-}\left\{1+F_-\ \exp\left(\frac{2iX}{\xi_-}\right)\right\}\right], \tag{27}$$

$$F_\pm=\frac{|\Delta_\pm|}{E}\,\frac{(1-\sigma_N)\Gamma_\mp\ \exp(i\varphi_- - i\varphi_+)-\Gamma_\pm}{1+(\sigma_N-1)\Gamma_+\Gamma_-\ \exp(i\varphi_- - i\varphi_+)},$$

$$\xi_\pm=\frac{\hbar^2 k_{\mathrm{FS}}\cos\theta_S}{m\Omega_\pm}. \tag{28}$$

By comparing Eq. (26) with Eq. (19), $\rho_T(E,X)$ is regarded as the expectation value of $\rho(E,X)$ with the probability distribution 1. Figure 14 shows the calculated $\rho_T(E,X)$ for various X for the $d_{x^2-y^2}$-wave superconductor (ab-plane tunneling configuration) with $\alpha=\pi/4$. The peak at zero-energy level originates from the bound states at the I-S interface as discussed in the previous section. The inset shows the spatial dependence of zero-bias peak height [$=\rho_T(E=0,X)$]. It is easy to understand that the bound states are localized around the I-S interface, and they decay into the bulk with a length scale of coherent length $\xi_0[=\hbar^2 k_{\mathrm{FS}}/(m\Delta_1)]$.

We concentrate on LDOS at the I-S interface $\rho_0(E)[=\rho(E,X=0+)]$ which is expressed as

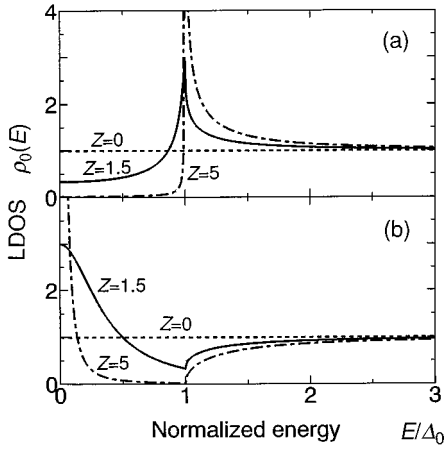

FIG. 15. Dependence of $\rho_0(E)$ on Z when (a) $\Delta_+=\Delta_-=\Delta_0$, and (b) $\Delta_+=-\Delta_-=\Delta_0$. The values of Z are set to 0, 1.5, and 5. As Z becomes larger, the peak structures are enhanced.

$$\rho_0(E)=\frac{1-(\sigma_N-1)^2|\Gamma_+\Gamma_-|^2}{|1+(\sigma_N-1)\Gamma_+\Gamma_-\ \exp(i\varphi_- - i\varphi_+)|^2}. \tag{29}$$

Figure 15 shows the dependence of $\rho_0(E)$ on Z when (a) $\Delta_+=\Delta_-=\Delta_0$ and (b) $\Delta_+=-\Delta_-=\Delta_0$. When $Z=0$, $\rho_0(E)$ shows a flat metallic behavior, which is completely different from that of $\sigma_R(E)$ as shown in Fig. 2. However, as Z becomes larger, the peak structures gradually grow and their forms become similar to those of $\sigma_R(E)$. The equation giving the energy level of the peaks in LDOS is obtained from the denominator of $\rho_0(E)$ which is equivalent to Eq. (23). This fact indicates that LDOS also has peaks at the energy level of the bound states (E_p). To see clearly the difference between $\rho_0(E)$ and $\sigma_R(E)$, the dependence of $\sigma_R(E)-\rho_0(E)$ on Z is shown in Fig. 16. When Z is small (≈ 0), the discrepancy is evident. However, as Z becomes larger, the difference becomes smaller except around $E=E_p$. This behavior is similar to that of Andreev reflection amplitude ($|a(E)|^2$) in Eq. (15). In fact, we obtain a relation for $E<|\Delta_-|$,

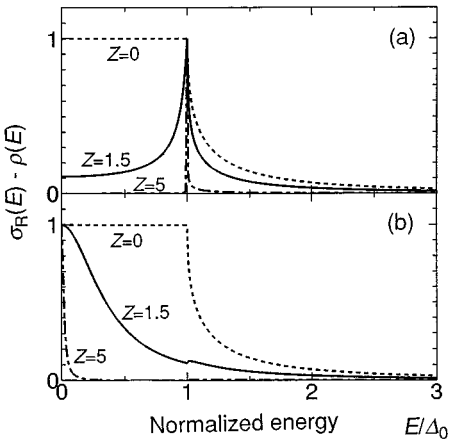

FIG. 16. Difference of LDOS and conductance spectra, $\sigma_R(E)-\rho_0(E)$, as a function of Z when (a) $\Delta_+=\Delta_-=\Delta_0$, and (b) $\Delta_+=-\Delta_-=\Delta_0$. The values of Z are set to 0, 1.5, and 5. As Z becomes larger, the difference becomes smaller except at $E=E_p$, where the difference is always 1 ($=|a(E_p)|^2$; see text).

$$\sigma_R(E)-\rho_0(E)=|a(E)|^2 = \frac{\sigma_N^2|\Gamma_+|^2}{|1+(\sigma_N-1)\Gamma_+\Gamma_- \exp(i\varphi_- - i\varphi_+)|^2} \quad (E<|\Delta_-|). \quad (30)$$

The peak heights of the two functions are $2(Z^2+1)$ for $\sigma_R(E_p)$ and $2Z^2+1$ for $\rho_0(E_p)$. The difference is just 1 $(=|a(E_p)|^2)$ independent of the barrier height.

In the limit of large barrier height, $\rho_0(E)$ converges to the surface DOS of isolated superconductor $\rho_S(E)$,

$$\rho_S(E)=\lim_{\sigma_N\to 0}\rho_0(E) = \frac{|\Delta_+\Delta_-|^2-|(E-\Omega_+)(E-\Omega_-)|^2}{||\Delta_+\Delta_-|-(E-\Omega_+)(E-\Omega_-)\exp(i\varphi_- - i\varphi_+)|^2}. \quad (31)$$

The $\rho_S(E)$ is equal to the BCS DOS when $\Delta_+=\Delta_-$. This fact indicates that the surface DOS agrees with that of the bulk only if $\Delta_+=\Delta_-$ is satisfied for all θ_S. In the limit of large barrier height, we can easily verify

$$\lim_{\sigma_N\to 0}\sigma_R(E)=\rho_S(E). \quad (32)$$

Apparently, Eq. (32) implies that, in this limit, the normalized conductance spectrum is sensitive to the surface DOS and insensitive to the depth profile inside the bulk of the superconductor. The information about the depth profile is indirectly reflected on the conductance spectra through the change of the surface DOS.

Finally, based on the above discussion, we obtain an approximated relation of the total tunneling conductance spectrum $\sigma_T(E)$. When the junction has sufficiently large barrier height (low conductance $\sigma_N\approx 0$), from Eqs. (21) and (32),

$$\sigma_T(E)\approx\frac{\int_{-\pi/2}^{\pi/2}d\theta_N\ \sigma_N\cos\theta_N\rho_S(E)}{\int_{-\pi/2}^{\pi/2}d\theta_N\ \sigma_N\cos\theta_N}. \quad (33)$$

Although $\rho_S(E)$ is given as a function of θ_S, the relation between θ_S and θ_N is explicitly given by Eq. (14). In most of the experimental situation, we implicitly assume $\sigma_N\approx 0$, and the conductance spectrum of the s-wave superconductor is assumed to coincide with the BCS DOS. Since the same assumption is used in the approximation of Eq. (33), this equation is applicable to most of the tunneling experiments. It is important to note that Eq. (33) is consistent with our intuition based on ''Golden rule,'' that is, in the large barrier-height limit, the total tunneling conductance spectrum $\sigma_T(E)$ converges to LDOS at the surface weighted by tunneling probability distribution $\sigma_N\cos\theta_N$. Of course, for s-wave superconductors, the effect of σ_N is negligible and then $\sigma_T(E)$ converges to the usual BCS DOS.

At this stage, we can analyze the experimental data based on Eq. (33). The most serious difficulty lies in the point how to estimate σ_N corresponding to the real experimental situation. By replacing E with $E+i\Gamma$ in Eqs. (27) and (28), we can introduce a possible lifetime broadening effect.[33] The finite value of Γ is sometimes convenient to avoid unphysical divergence of the peak.

VI. SUMMARY

In this paper the features and physics of tunneling conductance spectra are extensively investigated. The most important result is that the conductance spectra are sensitive not only to the amplitude but to the phase of pair potential. In the case of $d_{x^2-y^2}$-wave superconductors, the zero-energy conductance peaks are calculated in addition to the V-shaped gap structure. The physical origin of conductance peaks in the spectra is understood in terms of a quantized energy level formed between two different pair potentials. By comparing the conductance spectra with LDOS, we obtain an approximated equation that the conductance spectra converge to the LDOS weighted by a tunneling probability distribution in the large barrier-height limit.

The ZBCP's are widely observed in the tunneling experiments of high-T_c superconductors. We have investigated their origin in terms of the d-wave symmetry of the pair potential.[15] Further detailed comparison between the theory and experiments will elucidate important information about the electronic structures of high-T_c superconductors.

Through the study of the tunneling spectroscopy, it is shown that the anomalous bound states exist at the I-S interfaces of anisotropic superconductors. The existence of bound states seriously affect the electrical properties of Josephson junctions. This effect is investigated elsewhere.[34] Recently, the possibility of breaking time-reversal symmetry at the surface of $d_{x^2-y^2}$-wave superconductors is suggested.[35,36] Introduction of this effect into the calculation will strongly affect the conductance spectra, which will be carried out in the near future.

ACKNOWLEDGMENT

One of the authors (Y.T.) was supported by a Grant-in-Aid for Scientific Research in Priority Areas, ''Quantum Coherent Electronics, Physics and Technology,'' from the Ministry of Education, Science and Culture of Japan.

[1] M. Tinkham, *Introduction to Superconductivity* (McGraw-Hill, New York, 1975).
[2] E. L. Wolf, *Principle of Electron Tunneling Spectroscopy* (Oxford University Press, New York, 1985).
[3] A. Millis, D. Rainer, and J. Sauls, Phys. Rev. B **38**, 4504 (1988).
[4] C. Bruder, Phys. Rev. B **41**, 4017 (1990).
[5] D. A. Wollman, D. J. Van Harlingen, W. C. Lee, D. M. Ginsberg, and A. J. Leggett, Phys. Rev. Lett. **71**, 2134 (1993).
[6] C. C. Tsuei, J. R. Kirtley, C. C. Chi, L. S. Yu-Jahnes, A. Gupta, T. Shaw, J. Z. Sun, and M. B. Ketchen, Phys. Rev. Lett. **73**, 593 (1994).
[7] A. Mathai, Y. Gim, R. C. Black, A. Amar, and F. C. Wellstood, Phys. Rev. Lett. **74**, 4523 (1995).
[8] I. Iguchi and Z. Wen, Phys. Rev. B **49**, 12 388 (1994).

[9] T. Walsh, Int. J. Mod. Phys. B **6**, 125 (1992).
[10] J. Lesueur, L. H. Greene, W. L. Feldmann, and A. Inam, Physica C **191**, 325 (1992).
[11] S. Kashiwaya, M. Koyanagi, M. Matsuda, and K. Kajimura, Physica (Amsterdam) **194-196B**, 2119 (1994); S. Kashiwaya, M. Koyanagi, H. Takashima, H. Takashima, and K. Kajimura, *Advances in Superconductivity VI*, edited by T. Fujita and Y. Shiohara (Springer-Verlag, Tokyo, 1994), p. 73.
[12] Y. Koyama, Y. Takane, and H. Ebisawa, J. Phys. Soc. Jpn. (to be published).
[13] C. R. Hu, Phys. Rev. Lett. **72**, 1526 (1994); C. Yang and C. R. Hu, Phys. Rev. B **50**, 16 766 (1994).
[14] Y. Tanaka and S. Kashiwaya, Phys. Rev. Lett. **74**, 3451 (1995).
[15] S. Kashiwaya, Y. Tanaka, M. Koyanagi, H. Takashima, and K. Kajimura, Phys. Rev. B **51**, 1350 (1995).
[16] M. Matumoto and H. Shiba, J. Phys. Soc. Jpn. **64**, 1703 (1995).
[17] Y. Nagato and K. Nagai, Phys. Rev. B **51**, 16 254 (1995).
[18] Y. Tanaka and S. Kashiwaya (unpublished).
[19] G. E. Blonder, M. Tinkham, and T. M. Klapwidjk, Phys. Rev. B **25**, 4515 (1982).
[20] A. F. Andreev, Zh. Eksp. Teor. Fiz. **46**, 1823 (1964) [Sov. Phys. JETP **19**, 1228 (1964)].
[21] R. Landauer, Philos. Mag. **21**, 863 (1970).
[22] In the present paper, since we are interested in the normalized conductance, the factor in the conductance formulus is omitted.
[23] In Refs. 14 and 15, the factor $\cos\theta_N$ is not included in the integration formula. This factor should be added to calculate the X-axis component of the tunneling current.
[24] Y. Nagato, K. Nagai, and H. Hara, J. Low Temp. Phys. **93**, 33 (1993).
[25] I. O. Kulik, Zh. Eksp. Teor. Fiz. **57**, 1745 (1969) [Sov. Phys. JETP **30**, 944 (1970)].
[26] J. Bardeen and J. L. Johnson, Phys. Rev. B **5**, 72 (1972).
[27] A. Furusaki and M. Tsukada, Phys. Rev. B **43**, 10 164 (1991).
[28] S. Kashiwaya, Y. Tanaka, M. Koyanagi, and K. Kajimura, in *Advances in Superconductivity VII*, edited by K. Yamafuji and T. Morishita (Springer-Verlag, Tokyo, 1995), p. 45.
[29] S. Kashiwaya, Y. Tanaka, M. Koyanagi, and K. Kajimura, Jpn. J. Appl. Phys. **34**, 4555 (1995).
[30] P. G. de Gennes and Saint James, Phys. Lett. **4**, 151 (1963).
[31] Strictly, these are two types of bound states of which wave vectors have opposite signs to each other. Here, we only note the bound state condition conserving the momentum component parallel to the interface. See S. Kashiwaya, Y. Tanaka, M. Koyanagi, and K. Kajimura, J. Phys. Chem. Solids (to be published), and Ref. 29.
[32] Y. Tanaka and M. Tsukada, Phys. Rev. B **42**, 2066 (1990); **47**, 287 (1993).
[33] R. C. Dynes, V. Narayanamurti, and J. P. Garno, Phys. Rev. Lett. **41**, 1509 (1978).
[34] Y. Tanaka and S. Kashiwaya (unpublished).
[35] K. Kuboki and M. Sigrist (unpublished).
[36] M. Matsumoto and H. Shiba, J. Phys. Soc. Jpn. **64**, 3384 (1995).